PROCEEDINGS OF SPIE

SPIEDigitalLibrary.org/conference-proceedings-of-spie

Generalized analytical and numerical modeling of optical second harmonic generation in anisotropic crystals and complex heterostructures using #SHAARP package

Rui Zu, Bo Wang, Jingyang He, Lincoln Weber, Jian-Jun Wang, et al.

Rui Zu, Bo Wang, Jingyang He, Lincoln Weber, Jian-Jun Wang, Long-Qing Chen, Venkatraman Gopalan, "Generalized analytical and numerical modeling of optical second harmonic generation in anisotropic crystals and complex heterostructures using #SHAARP package," Proc. SPIE 12681, Ultrafast Nonlinear Imaging and Spectroscopy XI, 1268106 (5 October 2023); doi: 10.1117/12.2676223



Event: SPIE Optical Engineering + Applications, 2023, San Diego, California, United States

Generalized Analytical and Numerical Modeling of Optical Second Harmonic Generation in Anisotropic Crystals and Complex Heterostructures Using #SHAARP Package

Rui Zu,^{a,1} Bo Wang^{a,e,1}, Jingyang He^a, Lincoln Weber^a, Jian-Jun Wang^a, 1, Long-Qing Chen^{a,c,d,†}, Venkatraman Gopalan^{a,b,c,*}

^aDepartment of Materials Science and Engineering, The Pennsylvania State University, University Park, PA USA 16802;
 ^bDepartment of Physics, Pennsylvania State University, University Park, PA USA 16802;
 ^cDepartment of Engineering Science and Mechanics, The Pennsylvania State University, University Park, PA USA 16802;
 ^dDepartment of Mathematics, The Pennsylvania State University, University Park, PA USA 16802;
 ^eMaterials Science Division, Lawrence Livermore National Laboratory, Livermore, CA USA 94550

*vxg8@psu.edu †lqc3@psu.edu

¹These authors contribute equally to this work

ABSTRACT

Optical second harmonic generation (SHG) is a nonlinear optical effect widely used for nonlinear optical microscopy and laser frequency conversion. The closed-form analytical solution of the nonlinear optical responses is essential for evaluating the optical responses of new materials whose optical properties are unknown a priori. Many approximations have therefore been employed in the existing analytical approaches, such as slowly varying approximation, weak reflection of the nonlinear polarization, transparent medium, high crystallographic symmetry, Kleinman symmetry, easy crystal orientation along a high-symmetry direction, phase matching conditions and negligible interference among nonlinear waves, which may lead to large errors in the reported material properties. To avoid these approximations, we have developed an open-source package named Second Harmonic Analysis of Anisotropic Rotational Polarimetry (\$SHAARP) for single interface (si) and in multilayers (ml) for homogeneous crystals. The reliability and accuracy are established by experimentally benchmarking with both the SHG polarimetry and Maker fringes predicted from the package using standard materials. SHAARP.si and SHAARP.ml are available through GitHub https://github.com/Rui-Zu/SHAARP and <a href="https://github.com/Rui-Zu/SHAARP.ml, respectively.

Keywords: Nonlinear Optics, Second Harmonic Generation, Materials Science, Modeling

1. INTRODUCTION

Since the discovery of coherent light sources in the 1960s, nonlinear optics have attracted significant interest in a wide range of applications, such as sensing, communication, wavelength conversion, surface chemistry, medical treatment, and biological and tissue imaging. In the recent two decades, quantum communication and quantum computing have leveraged nonlinear optics. Second harmonic generation (SHG) is a second-order nonlinear optical process that converts two photons at lower energy to a single photon at twice the photon energy. Electric-dipole optical SHG is defined as $P^{2\omega} = \varepsilon_0 \chi^{(2)} E^{\omega} E^{\omega}$, where $\chi^{(2)}$ is the intrinsic nonlinear optical susceptibility tensor that converts two electric fields, E^{ω} , at ω frequency to a nonlinear polarization, $P^{2\omega}$, at 2ω frequency. Since $\chi^{(2)}$ is a third-rank tensor, SHG has also been widely used as a sensitive probe of non-centrosymmetric structure and polar orders.

Characterizing absolute nonlinear coefficients requires precise modeling as well as reference material with known coefficients, such as Potassium dideuterium phosphate (KDP) or LiNbO₃. Since the early developed nonlinear optical models by Bloembergen & Pershan and Maker et al., ^{1,2} many research efforts have been devoted to developing comprehensive nonlinear optical models to precisely determine intrinsic nonlinear optical susceptibilities. However, due

Ultrafast Nonlinear Imaging and Spectroscopy XI, edited by Zhiwen Liu, Demetri Psaltis, Kebin Shi, Proc. of SPIE Vol. 12681, 1268106 © 2023 SPIE · 0277-786X · doi: 10.1117/12.2676223

to the complex wave mixing process, established models often adopt many assumptions to make the derivation tractable, such as high symmetry of studied materials, transparent media, and easy orientations. Since the discovery of polar metals, 3,4 traditional methods of obtaining absolute SHG coefficients are no longer accessible due to the strong absorption, lower symmetry, and naturally grown facets. Moreover, as more novel materials are discovered with variations in material properties, structures, number of interfaces, etc., a more generalized nonlinear optical model that can suit various material systems and probing conditions is in critical need. Thus, in this work, we have developed an open-source software package named \$SHAARP (Second Harmonic Analysis of Anisotropic Rotational Polarimetry) that can deliver both analytical and numerical nonlinear optical solutions in an on-demand modality. 5,6 \$SHAARP's results have been benchmarked by many well-studied materials systems, proving the high accuracy of \$SHAARP.

2. METHODOLOGY

Light propagations at the linear frequency (ω) inside an anisotropic medium are governed by the wave equation at the corresponding frequency, as shown below,

$$\nabla \times \nabla \times \mathbf{E}^{\mathrm{T},\omega} + \begin{pmatrix} \varepsilon_{L_{1}L_{1}}^{\omega} & \varepsilon_{L_{1}L_{2}}^{\omega} & \varepsilon_{L_{1}L_{3}}^{\omega} \\ \varepsilon_{L_{2}L_{1}}^{\omega} & \varepsilon_{L_{2}L_{2}}^{\omega} & \varepsilon_{L_{2}L_{3}}^{\omega} \end{pmatrix} \boldsymbol{\mu}^{\omega} \frac{\partial^{2}}{\partial t^{2}} \mathbf{E}^{\mathrm{T},\omega} = 0 \tag{1}$$
 where $\varepsilon_{L_{i}L_{j}}^{\omega}$ is the dielectric permittivity tensor at frequency ω in the lab coordinate system, and the $\boldsymbol{\mu}^{\omega}$ represents the

where $\varepsilon_{L_i,L_j}^{\omega}$ is the dielectric permittivity tensor at frequency ω in the lab coordinate system, and the μ^{ω} represents the magnetic permeability tensor at ω , which is assumed to be vacuum permeability μ_0 for a non-magnetic medium.⁷ Due to the nature of birefringence, the light can be decomposed into two rays with different displacement vectors $\mathbf{D}^{\mathbf{e},\omega}$ and $\mathbf{D}^{\mathbf{o},\omega}$, where superscript e and o are extraordinary and ordinary waves, respectively.

Optical SHG is a nonlinear optical effect due to the second-order nonlinear polarization in a material with broken-inversion symmetry, defined as

$$\mathbf{P}^{2\omega} = \varepsilon_0 \mathbf{\chi}^{(2)} \mathbf{E}^{\mathrm{T},\omega} \mathbf{E}^{\mathrm{T},\omega} \exp i(\mathbf{k}^{\mathrm{S}} \cdot \mathbf{r} - \omega t)$$
 (2)

where $P^{2\omega}$, $E^{T,\omega}$, $\chi^{(2)}$ are the nonlinear polarization at 2ω frequency, the electric field at ω frequency, and the SHG susceptibility. k^S is the wavevector of the source wave combining two electric fields at ω frequency. The nonlinear wave propagation is further governed by the wave equation at 2ω frequency, written as,

$$\nabla \times \nabla \times \mathbf{E}^{\mathrm{T},2\omega} + \begin{pmatrix} \varepsilon_{L_{1}L_{1}}^{2\omega} & \varepsilon_{L_{1}L_{2}}^{2\omega} & \varepsilon_{L_{1}L_{3}}^{2\omega} \\ \varepsilon_{L_{2}L_{1}}^{2\omega} & \varepsilon_{L_{2}L_{2}}^{2\omega} & \varepsilon_{L_{2}L_{3}}^{2\omega} \\ \varepsilon_{L_{3}L_{1}}^{2\omega} & \varepsilon_{L_{3}L_{2}}^{2\omega} & \varepsilon_{L_{3}L_{3}}^{2\omega} \end{pmatrix} \boldsymbol{\mu}^{2\omega} \frac{\partial^{2}}{\partial t^{2}} \mathbf{E}^{\mathrm{T},2\omega} = -\boldsymbol{\mu}^{2\omega} \frac{\partial^{2}}{\partial t^{2}} \mathbf{P}^{2\omega}$$

$$(3)$$

where $\varepsilon_{L_i,L_j}^{2\omega}$ represents the dielectric permittivity tensor at frequency 2ω in the lab coordinate system, and the $\mu^{2\omega}$ represents the magnetic permeability tensor at 2ω , assumed to be μ_0 .⁷ The general and particular solutions of Eq.(3), respectively, correspond to homogeneous and inhomogeneous waves. The number of different $P^{2\omega}$, depending on the number of interfaces and nonlinear optical mediums involved in the modeling, will result in the same number of inhomogeneous waves propagating in the mediums. The electric field of inhomogeneous waves can thus be expressed as,

$$\mathbf{E}^{S,2\omega} = \mathbf{C}^{S,2\omega} \exp i(\mathbf{k}^{S,2\omega}.\mathbf{r} - \omega t), \tag{4}$$

where $C^{S,2\omega}$ is the field strength to be determined from Eq. (3) for a given $P^{2\omega}$. The homogeneous waves, denoted as $k^{e,2\omega}$ and $k^{o,2\omega}$, can be evaluated in the same way as solving Eq.(1) but at 2ω frequency.

Solving boundary conditions is essential for evaluating both transmitted and reflected SHG intensities. The boundary conditions require the tangential components of wavevectors (k_{\parallel}) , electric fields (E_{\parallel}) and magnetic fields (H_{\parallel}) to be continuous across the interface. At linear frequency (ω) , the boundary conditions lead to Snell's law and Fresnel equations, as written below,

$$k_{L_1}^{I,\omega} = k_{L_1}^{R,\omega} = k_{L_1}^{T,\omega} = \left(k_{L_1}^{h,\omega}\right)_{M}, 1 \le i \le N$$
(5)

$$E_{\parallel}^{\mathrm{I},\omega} + E_{\parallel}^{\mathrm{R},\omega} = \left(\sum E_{\parallel}^{h,\omega}\right)_{\mathrm{M}_{2}} \tag{6}$$

$$\left(\sum E_{\parallel}^{h,\omega} \exp j\Phi^{h,\omega}\right)_{\mathbf{M}_{i}} = \left(\sum E_{\parallel}^{h,\omega}\right)_{\mathbf{M}_{i+1}}, 1 \le i \le N-1 \tag{7}$$

$$E_{\parallel}^{\mathrm{T},\omega} = \left(\sum E_{\parallel}^{h,\omega} \exp j\Phi^{h,\omega}\right)_{\mathrm{M}_{N}} \tag{8}$$

$$H_{\parallel}^{\mathrm{I},\omega} + H_{\parallel}^{\mathrm{R},\omega} = \left(\sum H_{\parallel}^{h,\omega}\right)_{\mathrm{M}_{2}} \tag{9}$$

$$\left(\sum H_{\parallel}^{h,\omega} \exp j\Phi^{h,\omega}\right)_{\mathbf{M}_{i}} = \left(\sum H_{\parallel}^{h,\omega}\right)_{\mathbf{M}_{i+1}}, 1 \le i \le N-1 \tag{10}$$

$$H_{\parallel}^{\mathrm{T},\omega} = \left(\sum H_{\parallel}^{h,\omega} \exp j\Phi^{h,\omega}\right)_{\mathrm{M}_{N}} \tag{11}$$

Here, superscripts I, R, and T are incident, reflected, and transmitted waves in the air, respectively. N represent the number of layers of the medium, and M_i is the i^{th} layer of the medium. Superscript h stands for the group of homogeneous waves, namely, eF, oF, eB, and oB, where e, o, F, and B are extraordinary, ordinary, forward propagating, and backward propagating. Φ and j respectively, stand for the phase accumulated from the top interface to the bottom interface in M_i and the imaginary unit $(j = \sqrt{-1})$.

Similarly, at the nonlinear frequency (2ω) , due to the absence of incident waves and the presence of nonlinear polarizations, a general boundary condition with all layers being SHG active can be expressed below,

$$k_{L_1}^{I,\omega} = k_{L_1}^{R,2\omega} = k_{L_1}^{T,2\omega} = \left(k_{L_1}^{h,2\omega}\right)_{M_i}, 1 \le i \le N$$
(12)

$$E_{\parallel}^{R,2\omega} = \left(\sum E_{\parallel}^{h,2\omega} + \sum E_{\parallel}^{S,2\omega}\right)_{M_2} \tag{13}$$

$$\left(\sum E_{\parallel}^{h,2\omega} \exp j\Phi^{h,2\omega} + \sum E_{\parallel}^{S,2\omega} \exp j\Phi^{S,2\omega}\right)_{\mathbf{M}_{i}} = \left(\sum E_{\parallel}^{h,2\omega} + \sum E_{\parallel}^{S,2\omega}\right)_{\mathbf{M}_{i+1}}, 1 \leq i \leq N-1 \tag{14}$$

$$E_{\parallel}^{\mathrm{T},\omega} = \left(\sum E_{\parallel}^{h,2\omega} \exp j\Phi^{h,2\omega} + \sum E_{\parallel}^{S,2\omega} \exp j\Phi^{S,2\omega}\right)_{\mathrm{M}_{N}} \tag{15}$$

$$H_{\parallel}^{\mathrm{R},2\omega} = \left(\sum H_{\parallel}^{h,2\omega} + \sum H_{\parallel}^{S,2\omega}\right)_{\mathrm{M}_{2}} \tag{16}$$

$$\left(\sum H_{\parallel}^{h,2\omega}\exp j\Phi^{h,2\omega}+\sum H_{\parallel}^{S,2\omega}\exp j\Phi^{S,2\omega}\right)_{\mathbf{M}_{i}}=\left(\sum H_{\parallel}^{h,2\omega}+\sum H_{\parallel}^{S,2\omega}\right)_{\mathbf{M}_{i+1}},1\leq i\leq N-1 \tag{17}$$

$$H_{\parallel}^{\mathrm{T},\omega} = \left(\sum H_{\parallel}^{h,2\omega} \exp j\Phi^{h,2\omega} + \sum H_{\parallel}^{S,2\omega} \exp j\Phi^{S,2\omega}\right)_{\mathrm{M}_{N}} \tag{18}$$

Equations (12) – (18) share the same definition of parameters as in Equations (5) – (11). Additionally, superscript S represents the group of source waves, namely, eFeF, eFoF, oFoF, eBeB, eBoB, oBoB, eFeB, eFoB, oFeB, oFoB. The source waves (S) are a combination of two waves at the linear frequency (ω). For example, the term eFoB represents the nonlinear source wave formed by the mixture of forward propagating extraordinary wave and backward propagating ordinary wave, and the corresponding wavevector is $\mathbf{k}^{eFoB,2\omega} = \mathbf{k}^{eF,\omega} + \mathbf{k}^{oB,\omega}$. Figure 1 summarizes the nonlinear wave schemes as described above. Figure 1a describes the nonlinear optical model with a single interface (\sharp SHAARP.si), where the M_1 is semi-infinite thick and has no backward propagating light contributing to the boundary conditions. A single interface can be applied to many cases, such as studying strongly absorbing materials and wedged samples. Thus, the reflected SHG intensity will be the primary focus when applying the single interface. For a more generalized case, examples such as thin films⁸, superlattices⁹, and quasi-phase-matching (QPM)¹⁰ will require multilayer models for the SHG analysis. Figure 1b demonstrates the ray diagrams used in the multilayer analysis in the \sharp SHAARP.ml package, where ml stands for multilayers.

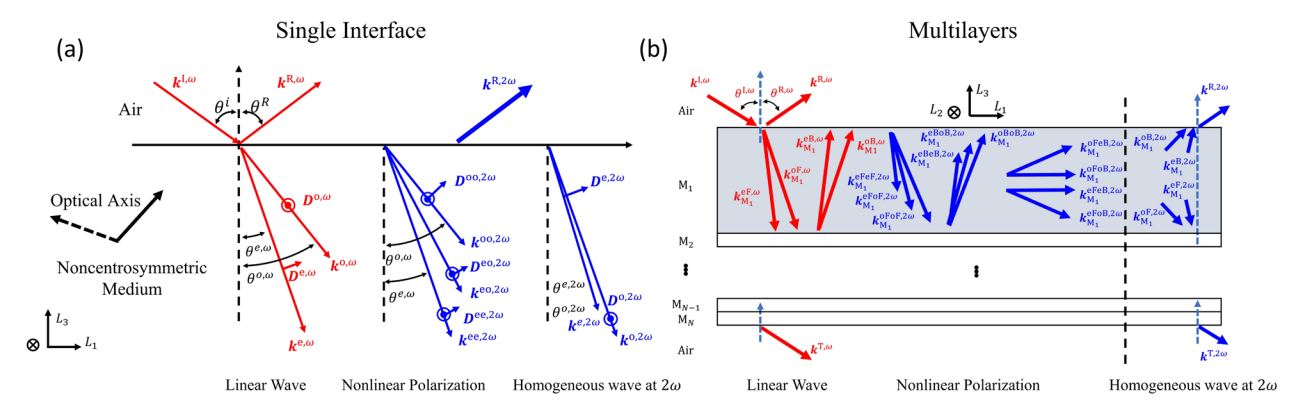


Figure 1. Ray diagrams used in \sharp SHAARP. (a) Summary of waves in the SHG process generated at the single interface. The dashed optical axis indicates a second optical axis in biaxial crystals. (b) Summary of waves in the multilayer structure. Blue rays are nonlinear optical waves. (L_1, L_2, L_3) is the lab coordinate system with the plane of incidence defined in the $L_1 - L_3$ plane.

3. \$\psi SHAARP, SECOND HARMONIC ANALYSIS OF ANISOTROPIC ROTATIONAL POLARIMETRY

With the most generalized SHG modeling approach described in the previous section, we have developed a series of open-source packages to streamline and facilitate nonlinear optical analysis. The #SHAARP packages, abbreviated for second harmonic analysis of anisotropic rotational polarimetry, contain two versions, namely #SHAARP.si and #SHAARP.ml, for addressing single interface and multilayer conditions, respectively. From a materials properties perspective, #SHAARP features in analyzing materials with arbitrary orientation, symmetry, birefringence, absorption, dispersion, number of SHG active layers, and number of interfaces. #SHAARP also features in handling various probing and measurement conditions, including an arbitrary polarization state of light (linear, circular, or elliptical), Maker fringes analysis, and polarimetry analysis. The analytical and numerical solutions provided by #SHAARP empower nonlinear optical analysis from optical simulation to experimental characterization of novel materials systems. Furthermore, the graphic-user-interfaces (GUI) of #SHAARP packages provide easy and direct access to the nonlinear optical solutions without the prerequisite of coding skills, as shown in Figure 2.

Three well-studied nonlinear optical materials from all three optical classes, i.e., GaAs, LiNbO₃, and KTiOPO₄ (KTP), are selected to benchmark the analysis. Excellent agreement has been achieved between this work and literature covering all three optical classes, both transparent and absorbing systems. This agreement suggests \sharp SHAARP can be applied to a broad range of material families and can carry out robust derivations and analysis. The first-experimental identified Weyl semimetal, TaAs (112), is further selected for the study, and near five-time difference in d_{33} is found, originating from misorientation in published literature. The robust analysis and user-friendly GUI of \sharp SHAARP are designed to promote the comprehensive SHG analysis in an on-demand modality, benefiting nonlinear optical studies in exploring new materials, understanding structural properties relations, and advanced optical system design. The software is freely available using Mathematica® and Wolfram Player®, where the latter does not require a license. The \sharp SHAARP packages are freely available to everyone through GitHub with links below,

#SHAARP.si:

GitHub: https://github.com/Rui-Zu/SHAARP
Documentation: https://shaarp.readthedocs.io/en/latest/

♯SHAARP.*ml*:

GitHub: https://github.com/bzw133/SHAARP.ml https://shaarpml.readthedocs.io/en/latest/

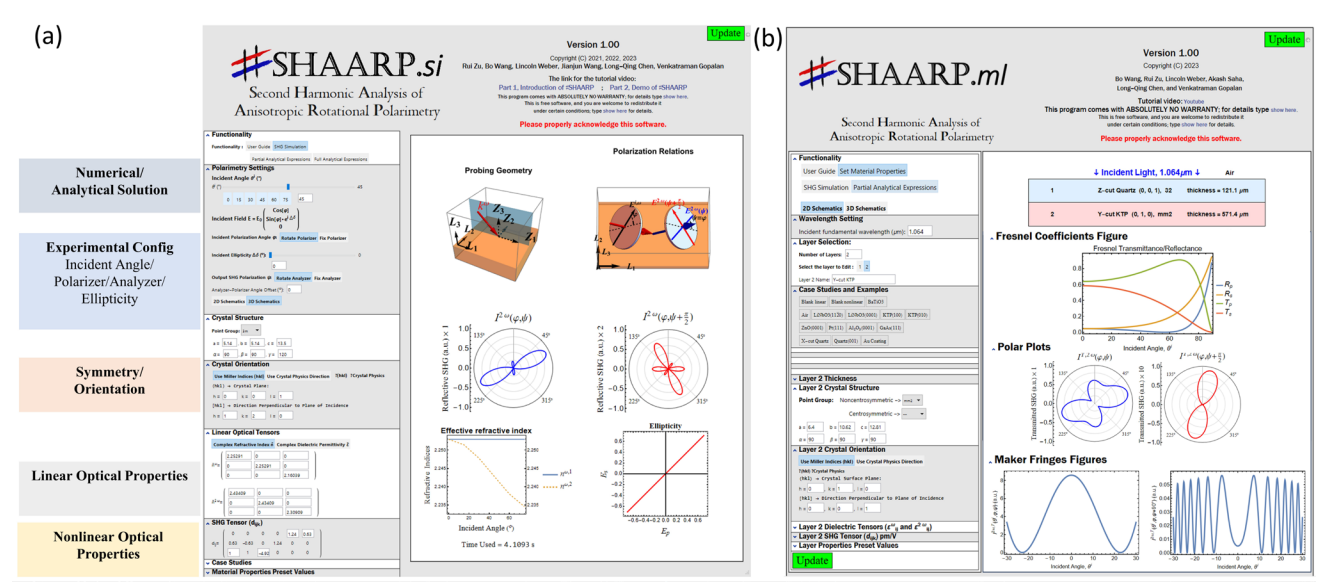


Figure 2. GUIs of \$SHAARP packages. (a) Simulation of Z-cut LiNbO₃ using \$SHAARP.si. (b) Simulation of a Z-cut Quartz//Y-cut KTP heterostructure using \$SHAARP.ml.

4. CONCLUSION

In summary, we have developed a comprehensive theoretical framework and open-source packages for nonlinear optical analysis, aiming to advance and unify the current theoretical understanding used for nearly seven decades, improve the precision and accuracy for numerical simulation, and enhance characterization capabilities toward new material systems that vary in their dimensionalities and properties. Two versions of #SHAARP are subsequently developed, namely #SHAARP.si (single interface) and #SHAARP.ml (multi layers), to fulfill the versatile material systems that are studied from materials that only one interface contributes to the obtained signal or mixed nonlinear optical response from a complex heterostructure. Ten essential features are addressed and integrated into #SHAARP, namely any number of interfaces, complete interference among waves, multireflection of waves at ω and 2ω frequencies, arbitrary materials properties including symmetry, orientation, absorption, birefringence and dispersion, polarization state of light, and flexible probing geometries. The #SHAARP packages are suitable for analyzing a broad range of materials, from single crystals to heterostructures. Looking forward, we believe the #SHAARP packages will benefit the nonlinear optical community.

Acknowledgment

The #SHAARP open-source package is supported by the US Department of Energy, Office of Science, Basic Energy Sciences, under Award Number DE-SC0020145 as part of the Computational Materials Sciences Program. R.Z., B.W., L.-Q.C., and V.G. were supported by the U.S. Department of Energy, Office of Science, Basic Energy Sciences, under Award No. DE-SC0020145. J.H. acknowledges support from National Science Foundation under NSF DMR-2210933. L.W. was supported by NSF Research Experiences for Undergraduates (REU), DMR 185-1987. Part of this work was performed under the auspices of the U.S. Department of Energy by Lawrence Livermore National Laboratory under Contract DE-AC52-07NA27344 (B.W.) R.Z. also received support from the NSF MRSEC Center for Nanoscale Science, DMR-2011839, for optical characterizations. R.Z. and V.G. acknowledge useful discussions with Dr. Zhiwen Liu. R.Z. acknowledges the analytical HH expressions from Sankalpa Hazra, the help with Au coating from Jeff Long and discussions with Dr. Yakun Yuan.

REFERENCES

- [1] Bloembergen, N. and Pershan, P. S., "Light Waves at the Boundary of Nonlinear Media," Physical Review **128**(2), 606–622 (1962).
- [2] Maker, P. D., Terhune, R. W., Nisenoff, M. and Savage, C. M., "Effects of Dispersion and Focusing on the Production of Optical Harmonics," Phys. Rev. Lett. **8**(1), 21–22 (1962).
- [3] Kim, T. H., Puggioni, D., Yuan, Y., Xie, L., Zhou, H., Campbell, N., Ryan, P. J., Choi, Y., Kim, J.-W., Patzner, J. R., Ryu, S., Podkaminer, J. P., Irwin, J., Ma, Y., Fennie, C. J., Rzchowski, M. S., Pan, X. Q., Gopalan, V., Rondinelli, J. M., et al., "Polar metals by geometric design," Nature 533(7601), 68–72 (2016).
- [4] Padmanabhan, H., Park, Y., Puggioni, D., Yuan, Y., Cao, Y., Gasparov, L., Shi, Y., Chakhalian, J., Rondinelli, J. M. and Gopalan, V., "Linear and nonlinear optical probe of the ferroelectric-like phase transition in a polar metal, LiOsO 3," Applied Physics Letters 113(12), 122906 (2018).
- [5] Zu, R., Wang, B., He, J., Wang, J.-J., Weber, L., Chen, L.-Q. and Gopalan, V., "Analytical and numerical modeling of optical second harmonic generation in anisotropic crystals using \$\$SHAARP package," 1, npj Comput Mater 8(1), 1–12 (2022).
- [6] Zu, R., Wang, B., He, J., Weber, L., Saha, A., Chen, L.-Q. and Gopalan, V., "Optical Second Harmonic Generation in Anisotropic Multilayers with Complete Multireflection Analysis of Linear and Nonlinear Waves using #SHAARP.ml Package," arXiv:2307.01368 (2023).
- [7] Yariv, A., Yariv, P. of E. E. A., Yeh, P. and Yeh, P., [Optical Waves in Crystals: Propagation and Control of Laser Radiation], Wiley (1984).
- [8] Zu, R., Ryu, G., Kelley, K. P., Baksa, S. M., Jacques, L. C., Wang, B., Ferri, K., He, J., Chen, L.-Q., Dabo, I., Trolier-McKinstry, S., Maria, J.-P. and Gopalan, V., "Large Enhancements in Optical and Piezoelectric Properties in Ferroelectric Zn1-xMgxO Thin Films through Engineering Electronic and Ionic Anharmonicities," arXiv:2304.14532 (2023).
- [9] Stoica, V. A., Laanait, N., Dai, C., Hong, Z., Yuan, Y., Zhang, Z., Lei, S., McCarter, M. R., Yadav, A., Damodaran, A. R., Das, S., Stone, G. A., Karapetrova, J., Walko, D. A., Zhang, X., Martin, L. W., Ramesh, R., Chen, L.-Q., Wen, H., et al., "Optical creation of a supercrystal with three-dimensional nanoscale periodicity," 4, Nat. Mater. **18**(4), 377–383 (2019).
- [10] Boyd, R. W. and Prato, D., [Nonlinear Optics, 3 edition], Academic Press, Amsterdam; Boston (2008).
- [11] Wu, L., Patankar, S., Morimoto, T., Nair, N. L., Thewalt, E., Little, A., Analytis, J. G., Moore, J. E. and Orenstein, J., "Giant anisotropic nonlinear optical response in transition metal monopnictide Weyl semimetals," Nature Physics 13(4), 350–355 (2017).